セラミックス基盤工学研究センター年報 (2006). Vol. 6, 12 -18

電子密度分布解析用高温単結晶 X 線回折システムの開発

石澤伸夫 † ・近藤早 † ・日比野寿 † ・五十嵐眞悦 ‡ ・中村光雄 ¶ ・佐保良二 ¶

† 名古屋工業大学セラミックス基盤工学研究センター　〒 507-0071 岐阜県多治見市旭ヶ丘 10-6-29

‡ ブルカー・エイエックスエス (株)　〒 221-0022 神奈川県横浜市神奈川区守屋町 3-9-A

¶ 日本サーマルエンジニアリング (株) 〒 229-1132 神奈川県相模原市橋本台 1-6-2

Development of High-Temperature Single-Crystal X-ray Diffraction System for Electron Density Distribution Analyses

N. Ishizawa†, S. Kondo†, H. Hibino†, S. Igarashi‡, M. Nakamura¶ and R. Saho¶

† Ceramics Research Laboratory, Nagoya Institute of Technology, 10-6-29, Asahigaoka, Tajimi 507-0071

‡ Bruker AXS K. K., 3-9-A, Moriya-cho, Kanagawa-ku, Yokohama 221-0022

¶ Japan Thermal Engineering Co., Ltd., 1-6-2, Hashimotodai Sagamihara 229-1132

A new high-temperature diffraction system has been developed to collect accurate and precise single-crystal diffraction data at high resolution levels. The high-temperature apparatus is composed of two devices of a hot nitrogen gas blower and its duct which are located very close to the specimen so as to avoid heat dissipation to the other parts. The apparatus is attached to the CCD diffractometer to enable fast data collection at high temperatures up to over 1000 ºC with a stability of less than 1 ºC. The apparatus places no geometrical restriction to the diffractometer, allowing measurements up to 120º in 2θ. High temperature diffraction data were collected for the α-Al2O3 single crystal at 300, 600 and 900 ºC within 3 hours for each measurements. The merge R factors were less than 0.019 and the final agreement factors between Fo and Fc were less than 0.031 in the range $1^\circ < 2\theta < 92^\circ$. The Al atom was found to be gradually displaced with increasing temperature so that the Al-Al repulsion force across a pair of face-sharing octahedra can relax. The system will contribute to the electron density studies of functionally important inorganic materials at elevated temperatures.

[Received February 5, 2007; Accepted March 9, 2007]

1. Introduction

There has been an increasing demand to determine accurate electron density distribution and atom structures of crystalline materials at high temperatures in order to understand their physical properties. Recent development of area detectors and its integration with the single crystal diffractometer is achieving a marvelous success in obtaining data in much shorter time than the conventional point-detector diffractometer system. This is a great advantage in high-temperature diffraction experiments where the thermal degradation of crystals can often occur.

In this paper we report a development of new high-temperature single-crystal diffraction system which can control specimen temperatures in the range between room temperature and slightly over 1000 ºC. The heating apparatus is originally designed for the χ-fixed CCD diffractometer (Bruker Smart Apex II). However, the apparatus is essentially independent of the diffractometer geometry and can be applicable to a wide range of diffractometers with both area- and point-type detectors. The present paper first describe the high temperature apparatus and secondly demonstrate an example of the fast measurement of diffraction data at high temperatures using α-Al_2O_3 (corundum) single crystal.

2. Basic concepts

On designing a high-temperature single-crystal diffraction system, there are many important points to be considered. As mentioned in the previous section, the fast measurement to avoid heat damage is essential. The adoption of area detector is most advantageous in this point.

The inorganic crystals have moderate diffracted in-

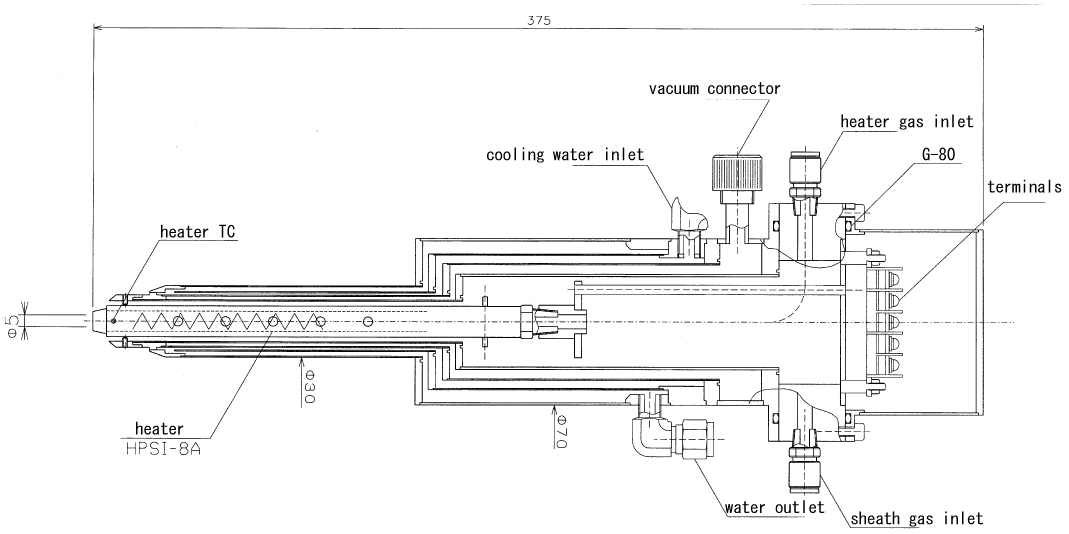

Fig. 1. Cross section of the hot gas blower.

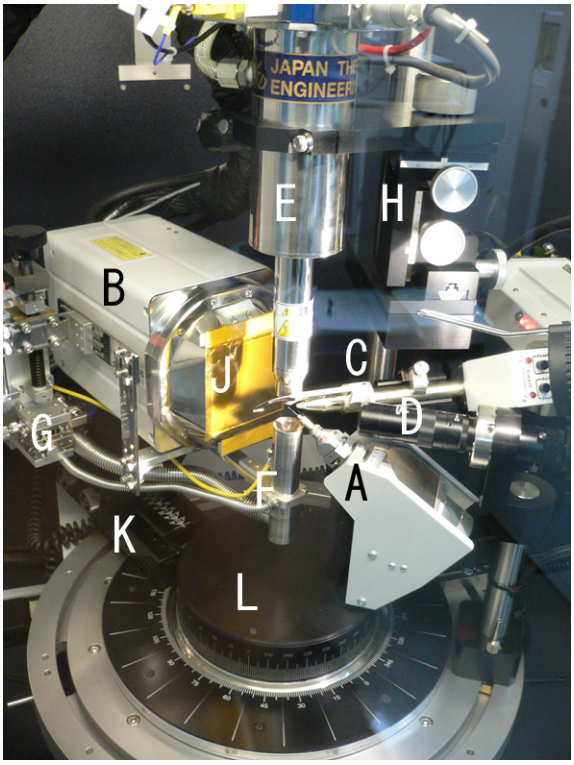

Fig. 2. A view of the high-temperature apparatus attached to the CCD diffractometer Smart Apex II. A: Chi cradle with goniometer head (Huber model 1004). B: CCD detector. C: total-reflection capillary collimator tube. D: microscope. E: Hot gas blower. F: Gas duct. G: xyz stage for positioning the gas duct. H: xyz stage for positioning the crystal heater. J: Polyimide film (Kapton film, DuPont) to protect detector window. K: Two-theta arm L: Omega stage

tensities even at high 2θ angles owing to the small thermal vibration of constituent atoms compared with the organic crystals. Data should be measured up to the upper limit of 2θ mechanically available for the diffractometer in order to carry out the electron density studies at high resolution levels. Merging high-angle frame data with low-angle ones used to be difficult in the past but now the problem has been almost solved in latest area-diffractometers.

Reconstruction of precession images from hundreds of frame data measured by the area detector is also essential to see what is going on in the crystal at high temperatures. This is especially the case when the crystal undergoes the phase transition or thermal decomposition. Because of the reasons above, the CCD diffractometer (Smart Apex II, Bruker AXS) was chosen as a base system.

The CCD detector is usually placed relatively close to the crystal to increase effective detection area in reciprocal space. This is especially the case for inorganic crystals with relatively small unit cells. The default distance is approximately 60 mm from the crystal in our diffractometer. The collimator and beamstop are also placed very close to the crystal to prevent air scattering. No large space in the CCD diffractometer is available for the heating apparatus compared with point detectors which usually has a crystal–detector distance of about 200 mm. Therefore the heat shield problem is of vital importance in designing the heating apparatus. In addition any geometrical restriction for the ω and φ move should

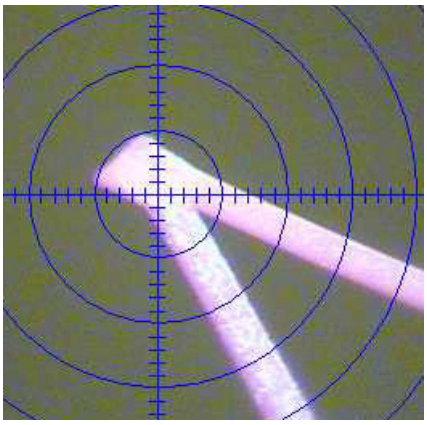

Fig. 3. K-type fine gauge thermocouple at the crystal position heated at 1000 ºC. The fine scale of the microscope is 20 μ m. The pink color reflects the bright Pt wire heater in the blower. See also Fig. 6 which shows a crystal instead of thermocouple with the same scale.

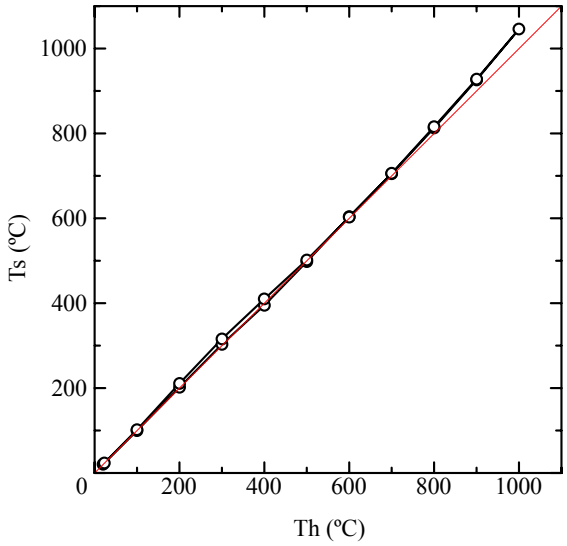

Fig. 4. Comparison between the temperatures of the heater (T_h) and the crystal position (T_s) .

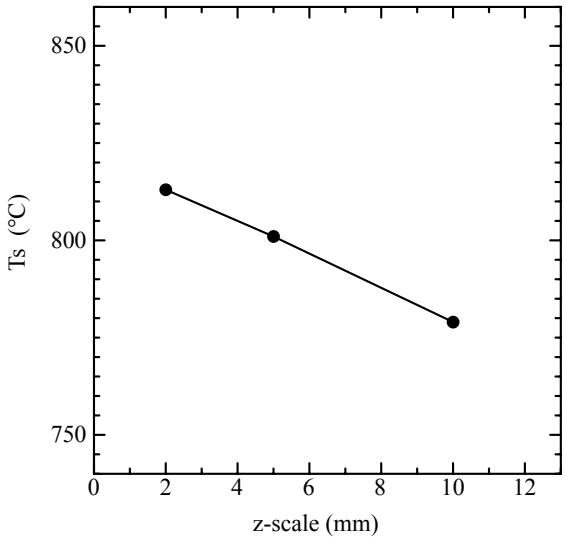

Fig. 5. Changes of temperature at the crystal position (T_s) as a function of nozzle position (T_h=800 ºC).

be avoided.

After various thoughts and trials, it was decided to employ a technique to elevate sample temperature by placing it in a hot gas stream. This technique can make an effective use of two spaces available for the χ-fixed CCD diffractometer, that is, a large space on top of the crystal and a small one just below it. The high-temperature attachment to the diffractometer is composed of two devices, a hot-gas blower and a gas duct. These devices are closely placed in the opposite sides of the crystal along the vertical line. A tight combination of the two devices in short distance enables a formation of a small columnar hot zone so that the heat diffusion to the other parts around the crystal can be minimized.

The diffraction intensities become weak due to thermal smearing at high temperatures. The incident X-rays should be intense enough to cope with the decay of diffracted intensities. The capillary optics based on the concept of total X-ray reflection (He & Preckwinkel, 2002) has been employed for the collimator in order to improve statistics of diffracted intensities.

3. The high-temperature apparatus

The cross section of the hot-gas blower is illustrated in Fig. 1. A platinum heater encapsulated in a silica glass tube heats the nitrogen gas (7 l/min) passing through the tube. The heater assembly is heat-shielded by multiple concentric walls for vacuum insulation and water-cooling. The heated gas comes out from the end opening of 5 mm in diameter of the silica glass tube. The sheath gas is supplied through the space between the silica glass tube and vacuum insulation tube. A constant flow of sheath gas (10 l/min) contributes to the formation of stable cool gas layer wrapping the hot gas stream and protects the equipment around the specimen; detector, collimator, beamstop, goniometer-head, etc.

The heat and sheath gases are supplied from a laboratory-type nitrogen gas generator (JAN3-08-MS, Japan Thermal Engineering Co., Ltd.), using the PSA (Pressure-Swing-Adsorption) technology. The temperature of the hot gas is measured by a Pt/Pt13%Rh thermocouple placed near the top (gas exit) of the blower nozzle, and

Table 1. Comparison of diffracted intensities of ylid between the total-reflection capillary collimator and the single-pinhole conventional collimator with 0.5 mm openings (Mo Kα tube).

capillary collimator					conventional collimator					gain
h	*k*	*l*	*I*	σ(*I*)	*h*	*k*	*l*	*I*	σ(*I*)	
0	-1	-5	30662	218	0	-1	-5	15917	154	1.926
0	-2	-7	2031	69	0	-2	-7	1103	51	1.842
0	-2	-8	1294	59	0	-2	-8	665	43	1.944
0	-3	-9	3410	106	0	-3	-9	1806	77	1.889
0	-3	-10	30403	323	0	-3	-10	15393	230	1.975
0	4	-3	25374	221	0	4	-3	12927	157	1.963
0	-4	-10	66	28	0	-4	-10	25	19	2.670
0	-4	-11	4587	139	0	-4	-11	2481	103	1.849
0	5	-3	1919	69	0	5	-3	953	49	2.014
0	-5	-11	8104	195	0	-5	-11	4194	141	1.932
0	-5	-12	31952	397	0	-5	-12	16624	285	1.922
0	6	-3	19902	237	0	6	-3	10189	170	1.953
0	-6	-12	5818	181	0	-6	-12	3108	132	1.872
0	-6	-13	1942	112	0	-6	-13	884	76	2.197
0	7	-3	308	38	0	7	-3	180	31	1.706
0	-7	-12	2229	123	0	-7	-12	1165	89	1.913
0	-7	-13	3304	150	0	-7	-13	1635	105	2.022

controlled by a PID (Proportional-Integral-Derivative) controller. The exhaust gas is immediately evacuated through the gas duct composed of flexible bellows-type concentric double tube made of stainless steel. The exhaust gas in the inner bellows tube is cooled by water running between the inner and outer tubes. The detector face is protected by the Polyimide (Kapton) film of 25 μm thick in case of unexpected scatter or evaporation of sample, ceramic adhesive, glasses, and /or heater materials.

4. Temperature calibration

The present apparatus can raise and hold the specimen temperature from room temperature to over 1000 ºC within the stability less than 0.5 ºC for long duration. The specimen temperature was examined by various methods. First the difference between the temperature (T_h) for power control and the temperature (T_s) at the specimen position was examined. The K-type fine sheet gauge thermocouple (KFC-50-200-100, Anbe SMT Co.) was placed at the crystal position as shown in Fig. 3. The junction of the thermocouple is 50 μm in size and 20 μm in thickness. The relation between T_h and T_s is plotted in Fig. 4. The plot points came close to the straight line with a unit slope, though T_s indicated slightly higher temperatures than T_h in general. This tendency became distinct with increasing temperature, especially above 800 ºC.

Sample temperature was also calibrated by measuring melting points of the metal crystals, Sn (m_p=231.9 ºC), Zn (m_p=419.5 ºC), and Ag (m_p=960.8 ºC). The melting of Pb and Ag crystals on heating was easily observed through the computer display connected to microscope with video output. The heater temperature (T_h) indicated 236 and 968 ºC on melting, respectively. The departure of Th from the true temperature was thus estimated to be approximately 4 ºC at 232 ºC and 7 ºC at 961 ºC. The Zn crystal was easily oxidized and covered by a tough ZnO skin, making difficult to observe the melting phenomenon through the microscope.

The effect of nozzle position on the temperature of specimen was examined. Changes of T_s at T_h = 800 ºC is given in Fig. 5. It should be noted that the horizontal axis of the figure reads the z-scale of the xyz stage of the heating nozzle directly. The crystal centre is displaced approximately 3 mm along z from the z = 0 position. Therefore the true distance between the crystal and the top of the heat nozzle can be obtained by adding 3 to the z-scale in mm. A significant temperature gradient along z existed. The temperature of the gas stream is estimated to be almost the same within the columnar hot zone. There-

Table 2. Data collection strategy at high temperatures. *S* is the total sweep angle about the scan axis.

Scan type	2θ (º)	ω (º)	φ (º)	*t* (s)	*w* (º)	*S* (º)
φ	-67.5	-122.50	-118.28	15.0	0.5	127.5
ω	-47.5	-88.54	325.00	10.0	0.5	34.0
ω	-27.5	-107.97	200.00	10.0	0.5	56.0
ω	57.5	-119.63	270.00	10.0	0.5	118.5

Table 3. Results of refinement I. Nref1 and Nref2 are the numbers of measured reflections and crystallographically independent ones with $I > 2\sigma(I)$, respectively. Rint is the merge R factor, and R is the reliability factor for the Nref2 reflections after the least-squares refinement. NR stands for 'not reported'. Data at 1900 ºC are imported from reference (Ishizawa et al., 1980).

T(ºC)	Nref1	$2\theta_{max}$	Rint	Nref2	R	a	c	Al z	O x
24	1581	120	0.0152	406	0.0190	4.7617(1)	12.9990(2)	0.352156(17)	0.69364(7)
300	535	92	0.0188	202	0.0304	4.7701(1)	13.0246(4)	0.35226(4)	0.69355(19)
600	537	92	0.0166	203	0.0245	4.7805(1)	13.0561(3)	0.35242(3)	0.69357(15)
900	529	92	0.0122	205	0.0227	4.7936(1)	13.0955(3)	0.35260(4)	0.69342(18)
1900	NR	60	NR	NR	0.0380	4.844(2)	13.27(2)	0.3533(2)	0.6936(1)

Table 4. Results of refinement II. Data at 1900 ºC are imported from reference (Ishizawa et al., 1980). NR stands for 'not reported'.

T(ºC)	Al U_{11}	Al U_{33}	Al U_{12}	Al Uiso
23	0.00305(7)	0.00370(8)	0.00152(3)	0.00327(6)
300	0.0071(2)	0.0059(2)	0.00356(12)	0.0067(2)
600	0.00832(19)	0.00866(19)	0.00416(10)	0.00843(16)
900	0.0108(2)	0.0122(2)	0.00540(11)	0.01126(19)
1900	0.0299(22)	0.0255(22)	NR	0.0285

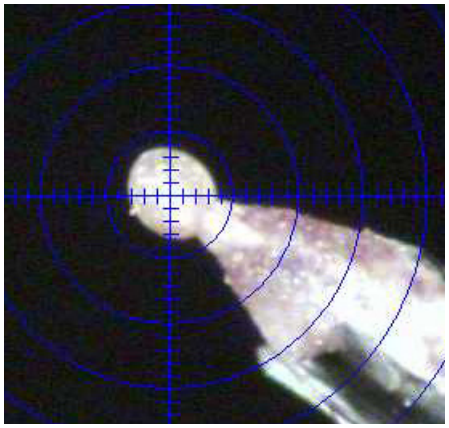

Fig. 6. Spherically-ground corundum crystal heated at 900 ºC. The fine scale of the microscope is 20 μ m.

Table 5. Results of refinement III. Data at 1900 ºC are imported from reference (Ishizawa et al., 1980). NR stands for 'not reported'.

T(ºC)	O U_{11}	O U_{22}	O U_{33}	O U_{12}	O U_{13}	O U_{23}	O Uiso
23	0.00358(8)	0.00380(10)	0.00430(10)	0.00190(5)	0.00035(3)	0.00070(7)	0.00387(6)
300	0.0078(3)	0.0081(3)	0.0065(3)	0.00405(17)	0.00064(10)	0.0013(2)	0.0074(2)
600	0.0087(2)	0.0089(3)	0.0095(2)	0.00446(14)	0.00091(8)	0.00181(15)	0.00902(17)
900	0.0108(3)	0.0117(3)	0.0132(3)	0.00586(17)	0.00114(10)	0.0023(2)	0.0118(2)
1900	0.0282(28)	0.0290(37)	0.0275(33)	NR	NR	0.0046(24)	0.0281

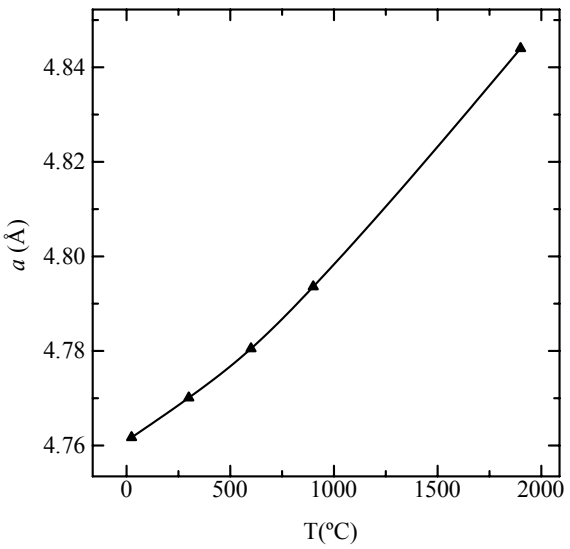

Fig. 7. Temperature dependence of the cell parameter a of corundum. Data at 1900 ºC are imported from reference (Ishizawa et al., 1980).

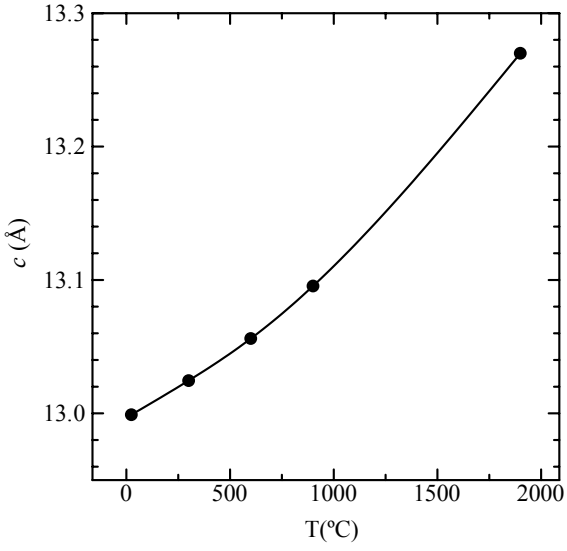

Fig. 8. Temperature dependence of the cell parameter c of corundum. Data at 1900 ºC are imported from reference (Ishizawa et al., 1980).

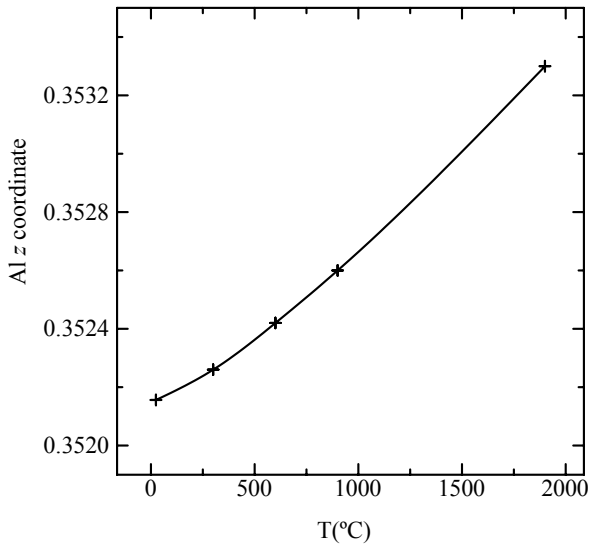

Fig. 9. Temperature dependence of the z parameter of Al in corundum. Data at 1900 ºC are imported from reference (Ishizawa et al., 1980).

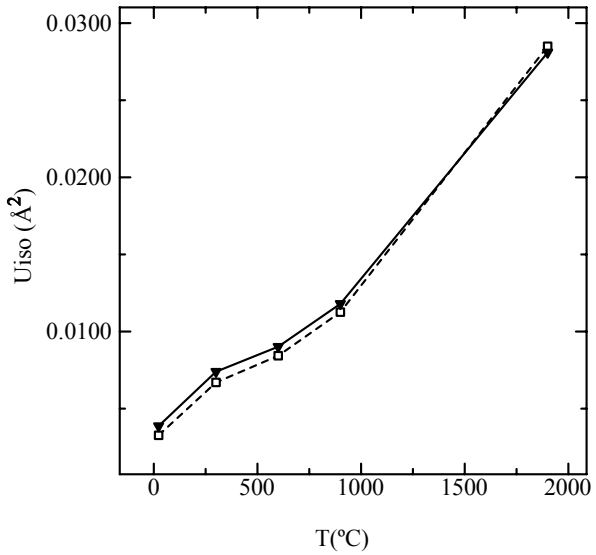

Fig. 10. Temperature dependence of isotropic atomic displacement parameters for Al (square) and O (triangle) of corundum. Data at 1900 ºC are imported from reference (Ishizawa et al., 1980).

fore, the observed gradient is supposedly caused by the radiation directly emitted from the platinum heater. It is important to confirm the nozzle position being set at the same position for each experiments.

5. Capillary optics of the collimator

The use of the total-reflection capillary collimator (RLR-173-0.5Cu(Mo), Bruker AXS) gave approximately twice as strong diffracted intensities compared with the single 0.5 Ø pinhole collimator. The integrated intensities and their estimated uncertainties of several reflections obtained from the standard crystal (ylid, $C_{11}H_{10}O_2S$) is given in Table 1. The average intensity gain was 2.02(3) for observed 171 reflections. It was confirmed from various room temperature preliminary experiments that the accuracy of the high angle data improved significantly by the use of capillary optics.

6. Corundum structure at high temperatures

The α-Al_2O_3 (corundum) single crystal was ground into a sphere of approximately 70 μm in radius by the Bond method. The crystal was mounted on a tapered silica glass capillary by the ceramic adhesive. The photograph of the crystal heated at 900 ºC is shown in Fig. 6.

Data were collected at 300, 600 and 900 ºC on heating, and 24 ºC after cooling. The strategy of data collection at high temperatures are optimized so that the total measurement time becomes approximately 3 hours, data completeness is close to 100% within $2\theta < 80º$, and redundancy of equivalent reflections is close to 3. The calculated strategy is given in Table 2.

The results of refinements are tabulated in Tables 3, 4 and 5 in the hexagonal setting. Changes of the a and c cell dimensions of α-Al_2O_3 with temperature are shown in Figs. 7 and 8, respectively. They increases as a function of temperature, and are smoothly extrapolated to data at 1900 ºC reported by Ishizawa et al., (1980). The unit cell structure of α-Al_2O_3 has two positional variables; z for Al and x for O. The fractional coordinate of Al z increased as a function of temperature as shown in Fig. 9. It was smoothly extrapolated to the value at 1900 ºC. On the other hand there was no significant systematic change in the O x parameter.

The temperature changes of the isotropic atomic displacement parameters (Uiso) of Al and O is shown in Fig. 10. A small convex at around 300 ºC was observed for both Al and O atoms. We think that this convex is simply an artefact due to low quality data of 300 ºC. Actually a large amount of the ceramic adhesive was observed in the virgin crystal mounted on the silica glass capillary. The precession images constructed from the frame data at 300 ºC showed a presence of strong powder rings due to the adhesive. The excessive adhesive evaporated completely after the measurement at 300 ºC. The powder rings became quite faint after that, resulting in a successful retrieval of integrated intensities from the 600, 900 and 24 ºC (on cooling) frame data. It is noted that as small amount of ceramic adhesive as possible should be

used for the precise and accurate data collection.

The α-Al_2O_3 structure contains a pair of AlO_6 octahedra sharing a face. The Al-Al distance along the *c* axis through the shared face is the shortest among all Al-Al distances. The increase of Al *z* fractional coordinate can be interpreted as a structural relaxation to accommodate the elongation of the shortest Al-Al distance at high temperatures, working in cooperation with the expansion of the unit cell. It is suggested that the electrostatic repulsion forces between higher valence atoms increase at high temperatures.

7. Conclusion

A new high-temperature single-crystal diffraction system has been developed. The high-temperature apparatus is composed of the gas blower and the gas duct which are located very closely to the sample to avoid heat diffusion. The apparatus is attached to the CCD diffractometer to enable fast data collection at high temperatures. The system also includes nitrogen gas generator from air and the power supply for the PID controlled platinum heater and various safeguards. The temperature can be raised from room temperature to over 1000 ºC. Single-crystal diffraction data were successfully collected for α-Al_2O_3 at 300, 600 and 900 ºC within only 3 hours for each. The results of refinements provided precious structural information about the systematic shift of Al position at high temperatures. The system will contribute for the precise and accurate electron density studies of functionally important inorganic materials at elevated temperatures.

Acknowledgements

This study was supported by grants-in-aid for Scientific Research No. 18206071 from the Ministry of Education, Culture, Sports, Science and Technology, Japan.

References

B. B. He and U. Preckwinkel (2002). *Advances in X-ray Analysis*, Volume 45, 332-337.

N. Ishizawa, T. Miyata, I. Minato, F. Marumo and S. Iwai (1980). *Acta Cryst*. *B***36**, 228-230.